

# Hydrogen Evaluation Technology and Material Design Technology for Suppressing Hydrogen Embrittlement of High-Tensile-Strength Steels

Dr. Makoto KAWAMORI\*<sup>1</sup> · Takuya HIRAMATSU\*<sup>1</sup> · Dr. Junichiro KINUGASA\*<sup>2</sup> · Takayuki YASUI\*<sup>3</sup> · Takuya KOCHI\*<sup>3</sup> · Yosuke FUJITA\*<sup>4</sup>

\*<sup>1</sup> Materials Research Laboratory, Technical Development Group

\*<sup>2</sup> Application Technology Center, Technical Development Group

\*<sup>3</sup> Wire Rod & Bar Products Development Department, Research & Development Laboratory, Steel & Aluminum Business

\*<sup>4</sup> Corrosion & Protection Evaluation Department, Material Solution Center, KOBELCO RESEARCH INSTITUTE, INC.

## Abstract

*Increasing the tensile-strength of steel is an effective means of reducing the weight of automobiles and the environmental burden. Kobe Steel has developed high-tensile-strength steel for bolts, springs, thin steel sheets, and other products and provided them to society. To meet the demands for even higher-tensile-strength and applications in severe corrosion and hydrogen environments, it is important to understand the factors influencing hydrogen embrittlement, which may be a challenge for high-tensile-strength steels, and to create material design technology. This paper introduces hydrogen evaluation technologies to clarify the effects of the environment, material, stress, and strain on hydrogen embrittlement, including hydrogen entry monitoring using hydrogen permeation technique, hydrogen evaluation technology in materials using thermal desorption spectrometry, and slow strain rate tensile technique, as well as hydrogen visualization technology using secondary ion mass spectrometry. In addition, examples of material design technology, such as hydrogen entry suppression by elemental addition and hydrogen embrittlement suppression utilizing microstructure control and compressive residual stress, are explained.*

## Introduction

Increasing the tensile-strength of steel is an effective way to reduce environmental burden by supporting lower material consumption and reduced weight of vehicles and other transportation equipment, curtailing CO<sub>2</sub> emissions. However, steel's susceptibility to hydrogen embrittlement tends to increase with increasing tensile-strength, making the suppression of hydrogen embrittlement an issue that must be addressed. Postulated mechanisms of hydrogen embrittlement include hydrogen-enhanced localized plasticity (HELP)<sup>1), 2)</sup>, hydrogen-enhanced decohesion (HEDE)<sup>3)</sup>, hydrogen-enhanced strain-induced vacancies (HESIV)<sup>4), 5)</sup>, and combinations of these mechanisms<sup>6)</sup>. **Fig. 1** shows a schematic diagram of the process leading to crack initiation by hydrogen embrittlement. Hydrogen

from the environment enters a material and is trapped, diffuses, and accumulates based on the material microstructure and stress/strain. Crack initiation and propagation then occur, resulting in fracture. When the amount of hydrogen that enters the material from the environment (hydrogen concentration entered from the environment  $H_e$ ) exceeds the maximum hydrogen concentration that will not result in fracture (critical hydrogen concentration  $H_c$ ), a value specific to each steel, cracking occurs due to hydrogen embrittlement.<sup>7), 8), 9)</sup> Hence, the environment, material, and stress affect each other. Furthermore, it is necessary to consider the effects of plastic strain in, for example, automotive parts (frame parts) made of stamped high-tensile-strength steel sheet or cold-headed non-heat-treated bolts. **Fig. 2** shows a schematic diagram of the factors affecting hydrogen embrittlement as well as hydrogen evaluation material design technologies. Suppressing hydrogen embrittlement and developing materials with excellent resistance to this phenomenon requires two main developments. First, it requires hydrogen evaluation technologies that uncover the effects of material, environment, and stress and strain. Second, it requires material design technologies centered around the mechanisms behind hydrogen embrittlement as revealed by such hydrogen evaluation technologies.

**Fig. 3** shows a schematic diagram of hydrogen evaluation technologies organized by spatial and temporal resolution. This paper describes examples of the technologies we developed for suppressing hydrogen embrittlement in high-tensile-strength steel: evaluation technology of hydrogen entry from the environment, evaluation technology of hydrogen in materials, stress and strain evaluation technology, and material design technology coordinated to these technologies.

## 1. Evaluation and control technologies of hydrogen entry from the environment

When planning to use high-tensile-strength steel for automotive components, it is important

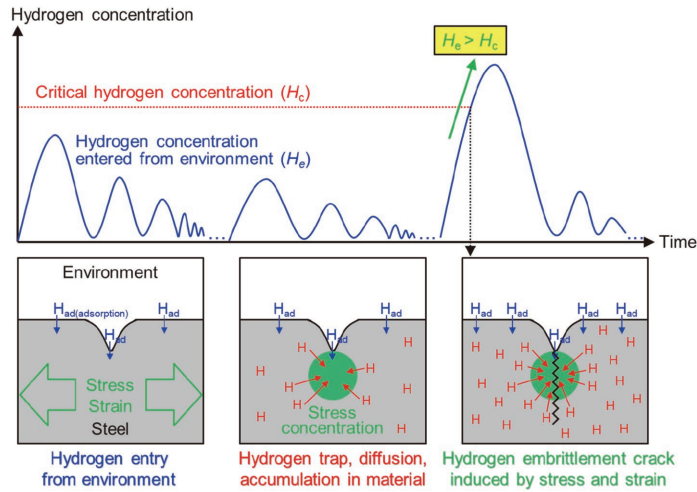


Fig. 1 Schematic illustration of process of hydrogen entry and crack initiation due to hydrogen embrittlement

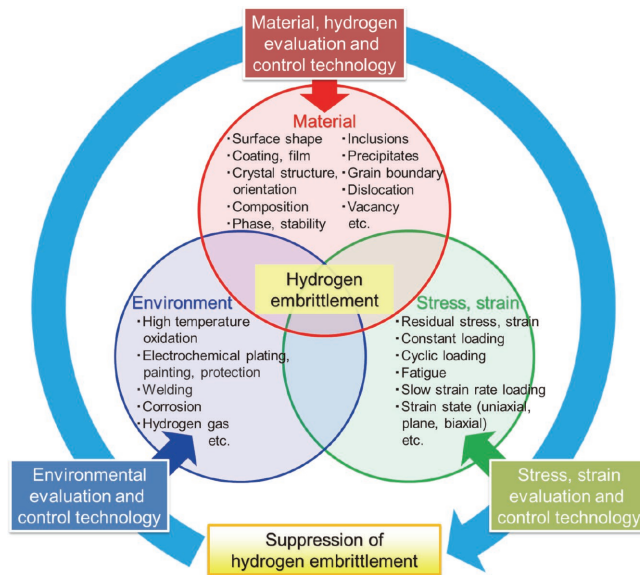


Fig. 2 Schematic illustration of factors affecting hydrogen embrittlement, hydrogen evaluation technology, and material design technologies

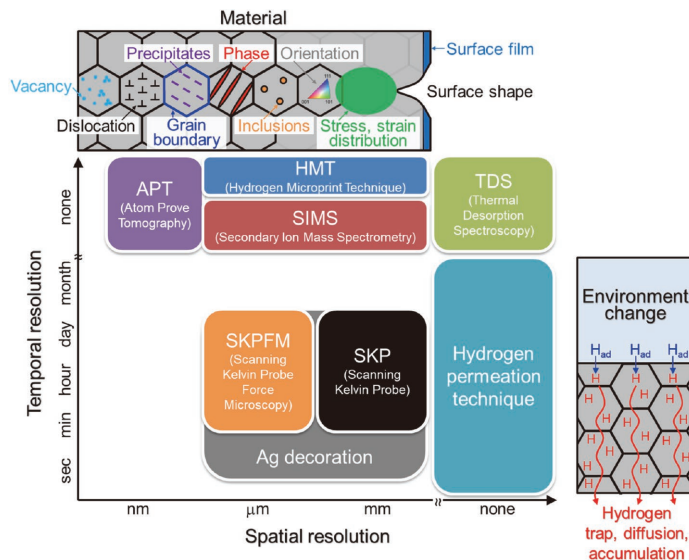


Fig. 3 Schematic illustration of spatial and temporal resolution of various hydrogen evaluation technologies

to understand the hydrogen concentration entered from the environment and the critical hydrogen concentration of the material, and to consider its applicability. As shown in Fig. 2, environmental factors that affect hydrogen entry are wide ranging and include manufacturing processes such as electrodeposition coating, and welding, as well as the vehicle operating environment. This section covers hydrogen entry in operating environments (corrosion environments) for which there is little understanding. It is difficult to determine the hydrogen concentration entered from a corrosion environment because hydrogen moves readily even at room temperature, so how the amount of hydrogen in steel changes over time is complex. Material samples that have fractured due to hydrogen embrittlement provide limited information of value because the exact time of fracture and the hydrogen concentration at that time are lost. Understanding the influence of the actual environment requires an in-depth grasp of hydrogen entry, the corrosion environment, and how fracture due to hydrogen embrittlement changes over time. Kobe Steel is developing various monitoring technologies accordingly. The hydrogen permeation technique is effective for long-term monitoring of hydrogen because, as shown in Fig. 3, it has a broader temporal resolution range than most other techniques. Further, this technique enables simple in-situ measurement. In the hydrogen permeation technique, hydrogen that has entered the steel is oxidized and detected as current. Fig. 4 shows examples of how we use evaluation technology of hydrogen entry from the environment. Kobe Steel has improved the hydrogen permeation technique such that long-term evaluation is possible even in particularly adverse corrosion environments. The use of temperature, humidity, and ACM (atmospheric corrosion monitoring) sensors for in-situ readings related to the environment and corrosion behavior in a corrosion environment elucidates the relationships between these factors and hydrogen entry. It is also possible to monitor the onset of hydrogen embrittlement by applying the strain gauge method to specimens replicating automotive parts (e.g., U-bend specimens to test bending workability). This test relates to actual vehicle operating environments and atmospheric corrosion environments. Here, we describe the application of this test to hydrogen entry into steel and hydrogen embrittlement behavior in an atmospheric corrosion environment.<sup>9), 10)</sup>

Japan covers many latitudes and thus many different climate zones, from subarctic Hokkaido in the north to subtropical Okinawa in the south.

This makes the country suitable for testing how an atmospheric corrosion environment affects hydrogen embrittlement in a broad sense. To investigate hydrogen embrittlement behavior in high-tensile-strength steel in subarctic, temperate, and subtropical climates, we conducted atmospheric exposure tests in Hakodate, Hokkaido; Choshi, Chiba Prefecture; and Miyakojima, Okinawa Prefecture, as shown in Fig. 4. For the hydrogen embrittlement evaluation, SCM435 steel sheets with a tensile-strength of 1,500 MPa and a thickness of 1.6 mm were used. U-bend specimens were prepared with a bending radius of 10 mm. To understand the material's behavior in terms of hydrogen embrittlement under stress, a bolt was threaded through the specimen, and a nut tightened down such that the strain measured by a strain gauge at the top of the bend was 4.9%.

Fig. 5 shows an analysis of the hydrogen embrittlement behavior through a comparison of the time-dependent change in the hydrogen concentration entered from the environment into the steel  $H_c$  with the critical hydrogen concentration  $H_c$ . The hydrogen concentration entered from the environment was calculated by the current from the hydrogen permeation technique using the steel's hydrogen diffusion coefficient using Fick's law.<sup>9)</sup> The U-bend specimens were immersed in aqueous solutions of varying pH values to study crack formation due to hydrogen embrittlement and determine the maximum amount of hydrogen at which cracking does not occur (critical hydrogen concentration  $H_c$ ) - see Fig. 5.<sup>9)</sup> In Miyakojima, which has abundant deleterious factors including high temperature and humidity, solar radiation, and sea salt, cracks due to hydrogen embrittlement were confirmed in the early stage of corrosion after the start of testing. By combining hydrogen embrittlement monitoring using the strain gauge method, hydrogen entry monitoring using the hydrogen permeation technique, and environmental monitoring using ACM sensors, it is possible to accurately determine the time of cracking, the amount of hydrogen that entered, and the specifics of the corrosion environment at that time. High ACM currents thought to be caused by rainfall were measured during the early stage of corrosion when cracking occurred due to hydrogen embrittlement. The corrosion reaction accelerated, resulting in increased hydrogen entry and cracking of the U-bend test specimen. The corrosion reaction accelerates and hydrogen entry increases not only in the early stage of corrosion, but also upon the deposition of airborne salt due to strong winds and typhoons that bring heavy rainfall. Choshi has

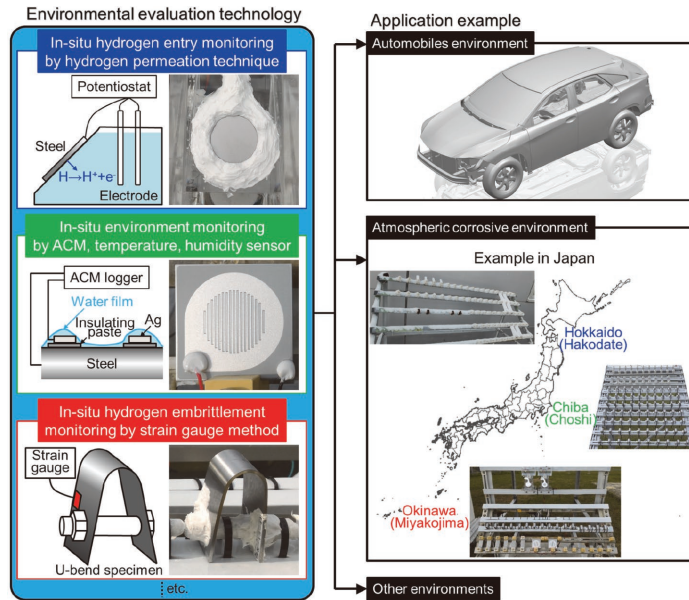


Fig. 4 Evaluation technology of hydrogen entry from the environment and monitoring technology of the environment and hydrogen embrittlement

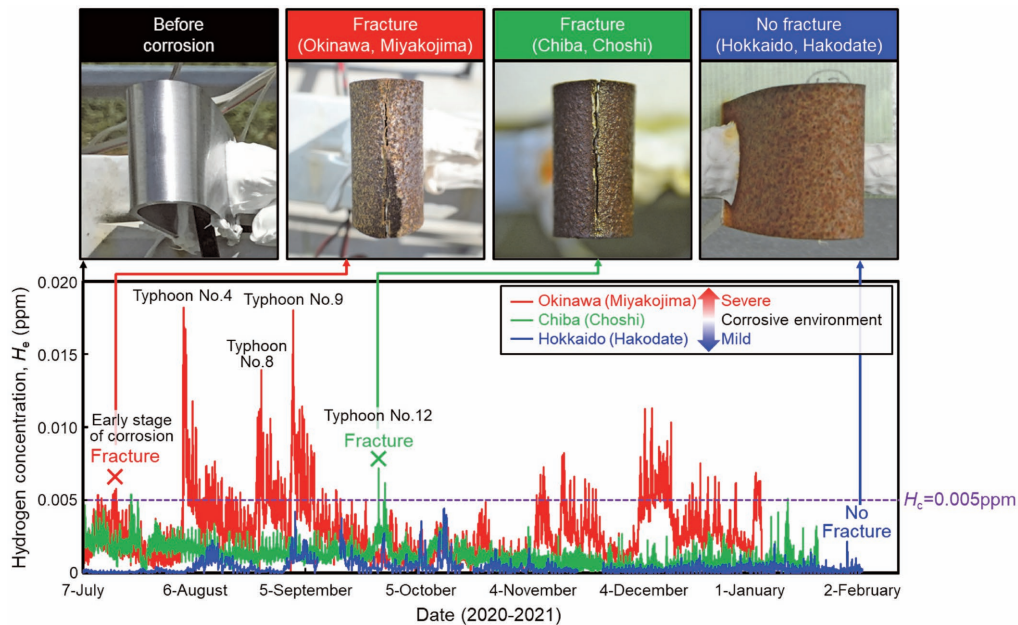


Fig. 5 Analysis of hydrogen embrittlement behavior based on comparison of time-dependent changes in hydrogen entry into steel in an atmospheric corrosion environment and the critical hydrogen concentration

a warm and humid climate and is representative of environmental exposure in Japan. In this test location, although the degree of hydrogen entry was insufficient to cause cracking under everyday conditions, the corrosion reaction accelerated upon the approach of a typhoon, increasing hydrogen entry as well as cracking due to hydrogen embrittlement. By contrast, Hakodate has a lower airborne salt content and lower temperature and humidity. Here, the amount of hydrogen entry was low because of the low amount of corrosion, and cracking due to hydrogen embrittlement did

not occur. As such, our monitoring and evaluation technology validated that the amount of hydrogen entry from the environment,  $H_e$  in an atmospheric corrosion environment, increases with an accelerated corrosion reaction due to airborne salt, rainfall, high temperature, and humidity. This technology also validated that when the amount of hydrogen entry from the environment  $H_e$  exceeds the critical hydrogen concentration  $H_c$ , cracking due to hydrogen embrittlement occurs. This technology can precisely evaluate hydrogen entry and hydrogen embrittlement behavior in actual environments and

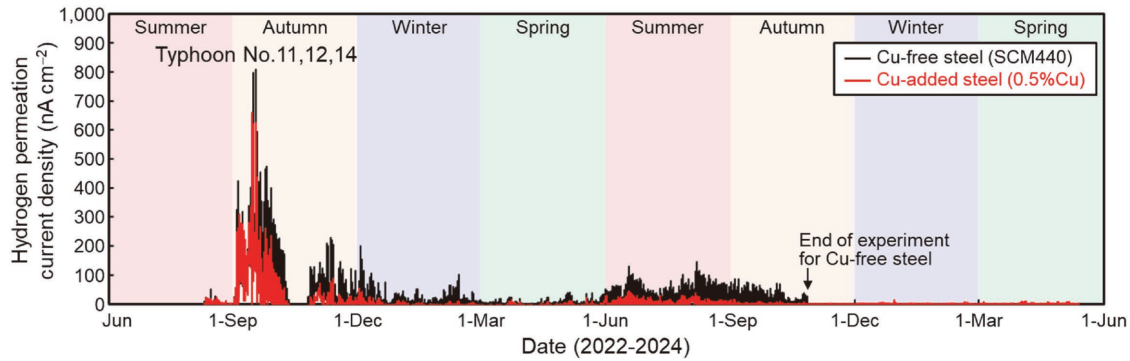


Fig. 6 Effect of Cu addition on hydrogen entry into steel in atmospheric corrosion environment

can be applied not only to the atmospheric corrosion environments described here, but also to vehicle operating environments, for example.

There is concern that hydrogen entry suppression methods that are not based on data from an actual environment might not be as effective as expected when used in an actual environment. Establishing and using the hydrogen environment evaluation technology described above enables the development of material design technology to suppress hydrogen entry in an actual environment.

As an example of hydrogen entry suppression technology in the form of adding elements to steel, Fig. 6 shows the effect of Cu on hydrogen permeation current density in an atmospheric corrosion environment. The hydrogen entry behavior of steel with 0.5% added Cu was compared with that of Cu-free SCM440 steel. Long-term hydrogen monitoring shows that adding Cu suppresses hydrogen entry in an actual environment. Furthermore, adding Ni reduces the hydrogen concentration entered from the environment<sup>11)</sup>, and adding Cu and Ni suppresses hydrogen embrittlement<sup>12)</sup>. Mechanisms behind these phenomena include improving the corrosion resistance of the base metal itself<sup>13)</sup>; suppressing the corrosion reaction through densification of rust<sup>12)</sup>, thereby reducing the generation of hydrogen; and inhibiting the driving force behind hydrogen entry caused by a higher electrical potential. Our hydrogen entry suppression technology has been applied to the development of high-tensile-strength steels for applications such as high-tensile-strength bolts and thin steel sheets<sup>14), 15)</sup>. We will continue to advance the development of countermeasures against hydrogen embrittlement in actual environments.

## 2. Evaluation and control technologies of hydrogen in materials

Vacancies, dislocations, grain boundaries, and

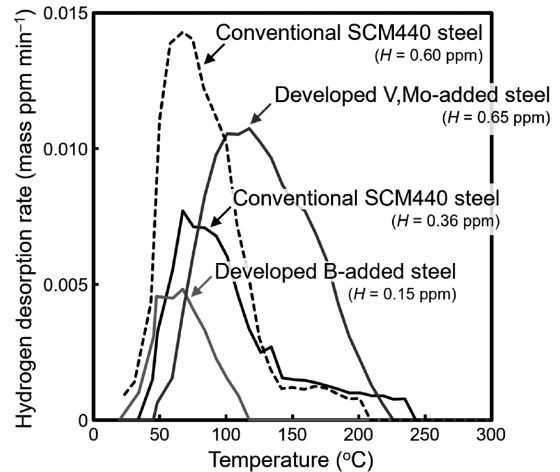


Fig. 7 Hydrogen desorption profile of conventional SCM440 steel, developed V, Mo-added steel, and developed B-added steel

precipitates are trapping sites for hydrogen entering a material from the environment. Additionally, the state of hydrogen changes with factors such as stress, strain, and material microstructure. It is important to evaluate and control the state of hydrogen in a material to suppress hydrogen embrittlement.

Thermal desorption spectroscopy (TDS) has become one of the most widely used methods for evaluating hydrogen in materials. TDS can quantitatively measure the concentration of hydrogen on the order of 0.01 ppm and yield a hydrogen desorption profile for evaluating the state of hydrogen. Fig. 7 shows an example of TDS results indicating the differing states of hydrogen for varying steel microstructures. Hydrogen was added to steel via cathodic charging method. The solid lines depict the hydrogen desorption profiles for different grades of steel upon hydrogen charging under the same conditions. The dotted hydrogen desorption profile is the result of charging more hydrogen at a higher current density than with the solid lines. The hydrogen desorption profiles for SCM440 steel with different hydrogen concentrations (0.36 ppm and 0.60 ppm) show that hydrogen is

trapped by relatively stable desorption sites on the high-temperature side and that as the hydrogen concentration increases, more desorption sites on the low-temperature side are occupied. Increasing the hydrogen concentration increases the amount of hydrogen that corresponds to desorption sites on the low-temperature side and that easily diffuses even at room temperature (diffusible hydrogen), accelerating hydrogen embrittlement.

Fig. 7 shows the hydrogen desorption profile of high-tensile-strength developed steel in which fine carbides containing V and Mo are dispersed by adding V and Mo and tempering at a high temperature of about 600°C. Compared with SCM440 steel, the peak is shifted toward the high-temperature side, indicating an increase in the number of stable, strong hydrogen trapping sites. Hydrogen was charged via cathodic charging method to annular notched specimens ( $K_t = 3.5$ ) of each steel grade with varying hardness as preparation for evaluating maximum nominal stress via the slow strain rate technique (SSRT)<sup>16)</sup> (results in Fig. 8). As the hardness of SCM440 steel increases, the maximum nominal stress after hydrogen charging decreases. The higher the tensile-strength, the more susceptible the steel is to hydrogen embrittlement.

In addition, intergranular fracture occurred near the crack initiation point, suggesting that this phenomenon was caused by hydrogen accumulation at the grain boundaries. However, the maximum nominal stress of V, Mo-added steel being higher than that of SCM440 steel of the same hardness indicates that the former has improved hydrogen embrittlement resistance. As shown in the hydrogen desorption profiles in Fig. 7, this may be due in

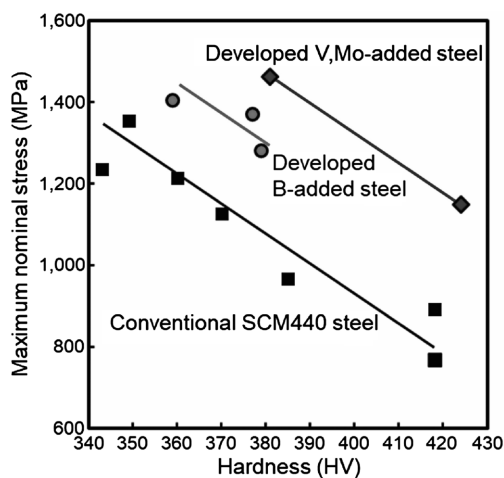


Fig. 8 Effect of hardness on the maximum nominal stress of conventional SCM440 steel, developed V, Mo-added steel, and B-added steel evaluated by SSRT after cathodic hydrogen charging method

part to the trapping of hydrogen by fine carbides containing V and Mo<sup>17)</sup>, suppressing hydrogen accumulation at the grain boundary. In addition to the hydrogen trapping effect, tempering at a high temperature reduces the number and mobility of dislocations, suppressing the transport of hydrogen to grain boundaries through dislocations. The spheroidization of grain boundary carbides further contributes to hydrogen embrittlement resistance.<sup>18)</sup> The use of V, Mo-added high-tensile-strength steel for bolts with excellent hydrogen embrittlement resistance reduces the size of automotive parts, thereby reducing vehicle weight and environmental burden, and enhances design flexibility.

Fig. 7 also shows the hydrogen desorption profile of the developed B-added steel. B-added steel is designed for high hardenability and high-tensile-strength grain boundaries through the replacement of relatively expensive Cr and Mo with B. The peak of B-added steel's hydrogen desorption profile is toward the low-temperature side in comparison with SCM440 steel, meaning that its hydrogen trapping power is less than or equal to that of conventional steel. However, at 0.15 ppm, the hydrogen concentration of the B-added steel is less than that of the SCM440 steel (0.36 ppm). As shown in the hydrogen embrittlement test results in Fig. 8, the B-added steel has a higher maximum nominal stress than SCM440 steel of the same hardness. It also has superior hydrogen embrittlement resistance, owing in part to the lower concentration of added elements such as Cr and Mo, which reduces the number of hydrogen trapping sites (amount of hydrogen entry), such as carbides. A further mechanism behind this benefit is the segregation of B to grain boundaries, which suppresses hydrogen accumulation at grain boundaries subjected to stress. Because the B-added steel is a lower alloy than SCM440 steel, it has better cold heading capacity. When used as steel for bolts, for example, the spheroidize annealing process before forming can be omitted, reducing costs and carbon emissions.

Our research validates TDS as an effective method for understanding the state of hydrogen to elucidate the mechanisms behind hydrogen embrittlement and develop material design guidelines for suppressing hydrogen embrittlement. We will improve the accuracy of our technology for determining the concentration of hydrogen via TDS alongside computational methods that can simulate the resulting hydrogen desorption profiles. This will improve the state of the art of technology for evaluating hydrogen in materials and support material design technology based on said technology.

### 3. Evaluation and control technologies of the effects of stress and strain

Hydrogen embrittlement is strongly influenced not only by the environmental and material factors mentioned above, but also by stress and strain. Hydrogen entering the material from the environment accumulates at stress concentration sites, promoting hydrogen embrittlement. In addition, dislocations and vacancies introduced by strain act as hydrogen traps and affect embrittlement through their interaction with hydrogen.<sup>19)</sup> Formed steel can have localized areas of high stress and strain. Therefore, to understand the parameters surrounding hydrogen embrittlement, it is necessary to understand how the localized hydrogen distribution changes based on the distribution of stress and strain. Although TDS is effective for determining the state of hydrogen in materials, it is ineffective for identifying the location of hydrogen in the material because it lacks spatial resolution (see Fig. 3). Hydrogen visualization techniques include atom probe tomography (APT), which has high spatial resolution at the atomic level<sup>20)</sup>, and the hydrogen microprint technique (HMT), which has superior sensitivity and resolution<sup>21)</sup> (Fig. 3). Hydrogen visualization techniques with both spatial and temporal resolution include the scanning Kelvin probe (SKP)<sup>22)</sup>, scanning Kelvin probe force microscopy (SKPFM)<sup>23)</sup>, and Ag decoration<sup>24)</sup>. Kobe Steel's research group is working to advance hydrogen visualization technology using secondary ion mass spectrometry (SIMS), which offers high spatial resolution covering the sub- $\mu$ m to sub-mm range as well as high sensitivity in the ppm to ppb

range for mass analysis.

As an example of hydrogen visualization technology for evaluating the effects of stress and strain, we introduce the results of an investigation into the hydrogen embrittlement mechanism of the U-bend test specimens.<sup>8), 25)</sup> Fig. 9 shows the fracture of the U-bend test specimen that underwent hydrogen embrittlement in the atmospheric corrosion environment (Miyakojima) shown in Fig. 5. The fracture near the outer surface of the bend was a quasi-cleavage fracture, whereas the fracture relatively farther from the surface was an intergranular fracture. We used SIMS to investigate the hydrogen distribution in the U-bend test specimen to understand the mechanism behind fracture development, the results of which are shown in Fig.10.<sup>8), 25)</sup> Here, deuterium (D) was used

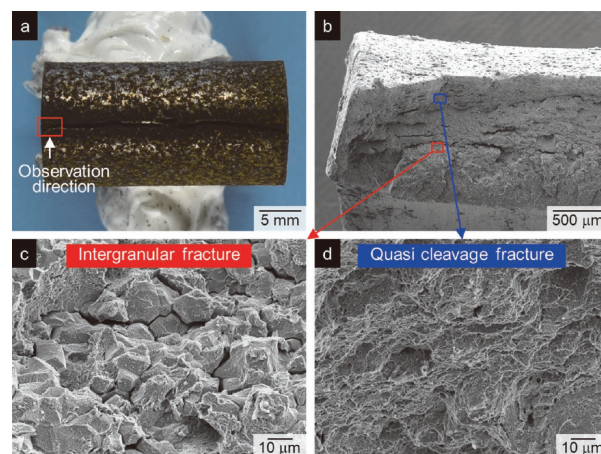


Fig. 9 (a) Photographic image and (b-d) SEM images of hydrogen embrittled U-bend specimens in atmospheric corrosion environment at Miyakojima, Okinawa

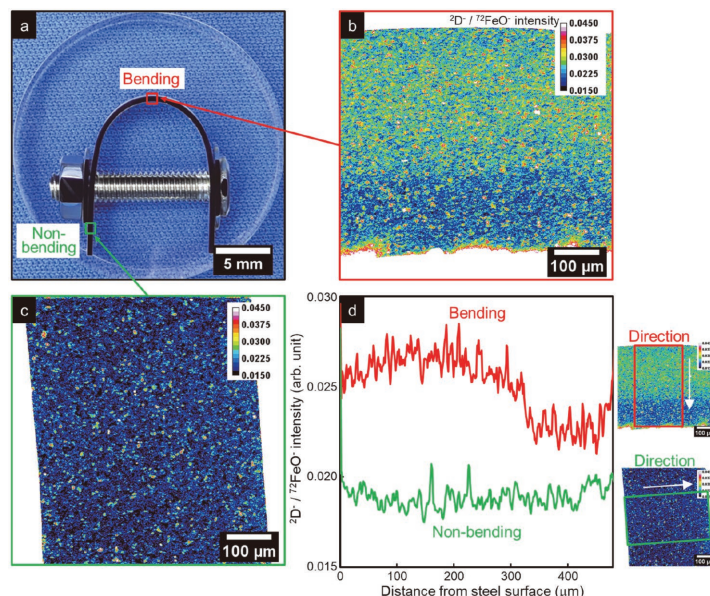


Fig.10 Deuterium visualization images of the U-bend specimen evaluated by SIMS

instead of hydrogen (H) as a tracer for hydrogen trapping sites. Isotope labeling using deuterium, a rare isotope, as a tracer makes it possible to differentiate hydrogen initially present in steel from deuterium introduced from the environment and to determine the locations of these isotopes. Furthermore, since it is possible to distinguish hydrogen in the sample from background hydrogen, the evacuation time required to reduce the background hydrogen can be shortened. This makes it possible to start evaluating the hydrogen visualization before the hydrogen in the specimen dissipates. More hydrogen was detected in the bending area of the U-bend specimen (Fig.10(b)) than in the non-bending area (Fig.10(c)). This was because the number of hydrogen trapping sites increased due to dislocations and vacancies introduced by the strain caused by bending. In the bending area, the hydrogen concentration was high on the front, where there is tensile stress, and low on the rear, where there is compressive stress. Further, the hydrogen concentration was highest about 0.1-0.2 mm into the outermost layer. This is because the highest compressive stress in the outermost layer occurs when the material is left as is in the spring-back state after bending, and when stress is then applied by tightening the bolt, the load is reduced by the compressive stress in the outermost layer, and the area inside the outermost layer becomes the area with the highest stress.

As shown in Fig. 9, intergranular and quasi-cleavage fractures were observed in the U-bend specimen. It has been reported that intergranular fracture occurs in areas of high local stress and hydrogen concentration.<sup>26)</sup> Quasi-cleavage fracture occurs readily in the presence of plastic deformation.<sup>27)</sup> It is believed that intergranular fracture occurred in the U-bend specimen with hydrogen embrittlement because of the high local hydrogen concentration resulting from the high localized stress some distance in from the surface. Because plastic deformation occurred near the surface, the dislocations and vacancies introduced interacted with hydrogen, resulting in quasi-cleavage fracture.

In the U-bend specimens, tensile stresses caused localized hydrogen accumulation and promoted hydrogen embrittlement. Described next is a case study in which shot peening was used to apply compressive stress to control the hydrogen distribution and suppress hydrogen embrittlement.<sup>28)</sup> Shot peening is a method of introducing plastic deformation. There is a concern that strain remaining on the surface of the steel after this process will increase the hydrogen concentration

by creating traps in the form of dislocations and vacancies. Therefore, low-temperature annealing was performed after shot peening to an extent that did not reduce compressive residual stress, with the objective of reducing the hydrogen concentration by stabilizing dislocations via Cottrell interaction with carbon and eliminating vacancies. In other words, the method was to suppress hydrogen embrittlement by reducing the amount of hydrogen trapped by strain while the surface of the steel is under compressive residual stress. Hydrogen visualization was then performed for the surface of the steel. A round bar test specimen of tempered martensitic steel with a tensile-strength of 2,000 MPa was subjected to cathodic hydrogen charging method on the surface that had been shot peened. Fig.11(a) shows the resulting hydrogen distributions as revealed via SIMS; Fig.11(b) shows the line profiles of hydrogen in the center and on the surface within a width of 50  $\mu\text{m}$ . In the non-shot-peened steel, the concentration of hydrogen in the surface layer is similar to that in the center, and hydrogen is trapped relatively uniformly inside the steel. Conversely, in the shot-peened steel, the concentration of hydrogen in the surface layer is less than that in the center, and there is no increase in hydrogen trapping due to the plastic strain introduced by shot peening. Hydrogen in the shot-peened steel decreases as the distance from the center to the surface layer increases, in parallel with the distribution of compressive residual stress.

We researched hydrogen embrittlement suppression technology using SIMS in conjunction with technology for evaluating the influence of stress and strain on hydrogen distribution. We evaluated the effects of shot peening on hydrogen embrittlement behavior by applying SSRT to hydrogen-charged round bar tensile test specimens. Fig.12 shows the findings, namely that shot peening increases the maximum nominal stress and hydrogen embrittlement resistance both when relatively large amounts of hydrogen were charged via cathodic charging method (Fig.12(a)) and when relatively small amounts of hydrogen were charged via the combined cyclic corrosion test (CCT) (Fig.12(b)). This is thought to be due to the relief of tensile stress via the compressive residual stress on the surface and due to reducing the concentration of hydrogen in the surface layer. In other words, it was revealed that the hydrogen embrittlement resistance can be improved by introducing compressive residual stress by shot peening and controlling the hydrogen distribution on the steel surface to a low level.

It will be increasingly important to reduce the

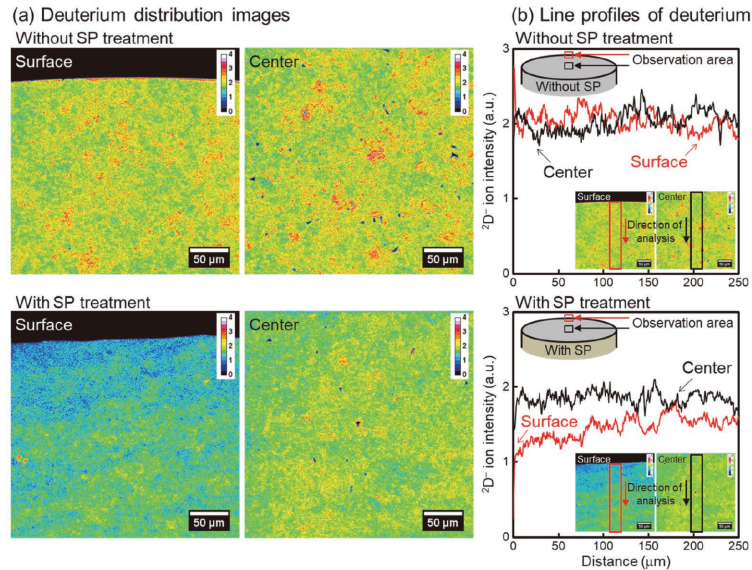


Fig.11 Effects of shot peening and subsequent low-temperature annealing on (a) deuterium distribution and (b) deuterium line profile in the surface and interior of steel

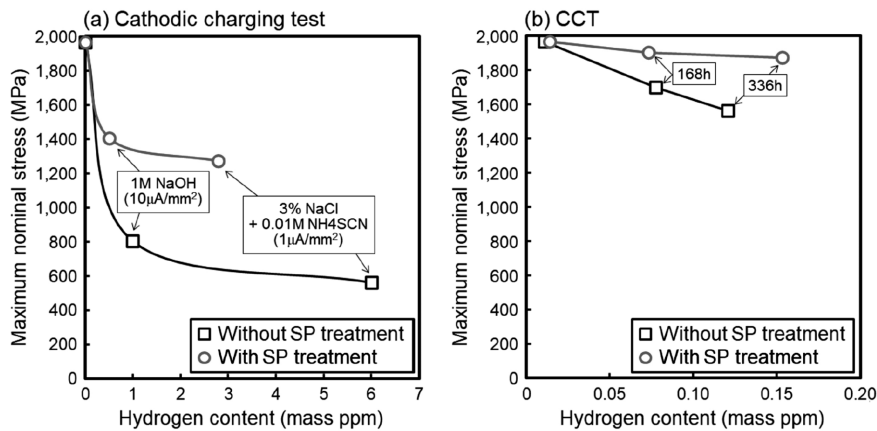


Fig.12 Effect of hydrogen concentration on the maximum nominal stress evaluated by SSRT of steels hydrogen-charged by (a) cathodic charging test and (b) combined cyclic corrosion test

need for heat treatment processes that release CO<sub>2</sub> emissions and to use high-tensile-strength steels formed by cold working to reduce environmental burden and processing. The technologies described here can be used to evaluate hydrogen embrittlement in high-tensile-strength materials under stress and strain after intense working. Further, these technologies support the development of guidelines for material design and production methods to suppress hydrogen embrittlement.

## Conclusions

This paper describes hydrogen evaluation and material design technologies for suppressing hydrogen embrittlement in high-tensile-strength steels. Materials that are designed for use in vehicles, conserve resources, and reduce environmental

burden are a necessity for fostering a safe, secure, low-carbon, recycling-oriented green society. To combat hydrogen embrittlement, it is critical to elucidate poorly understood aspects such as the effects of microstructure, residual stress, and processing strain on hydrogen entry and on the state and distribution of hydrogen in complex vehicle parts. We will improve environmental evaluation technologies for understanding and simulating the actual environments, technologies for evaluating hydrogen in materials with excellent spatial and temporal resolution, and technologies for measuring and controlling stress and strain. Such developments alongside our forthcoming prediction technologies rooted in computational science will advance hydrogen-resistant design technologies for materials. Through these technologies, we will foster the development of high-tensile-

strength steels such as bolt steels for automotive applications and ultra-high-tensile-strength thin steels to reduce environmental burden. In doing so, we will also develop materials for a hydrogen society, thereby contributing to a green society and to safe and security in community development and manufacturing.

## References

- 1) C. Beachem. Metallurgical Transactions. 1972, Vol.3, pp.441-455.
- 2) H. Birnbaum et al. Materials Science and Engineering: A. 1994, Vol.176, pp.191-202.
- 3) R. Oriani et al. Acta Metallurgica. 1974, Vol.22, pp.1065-1074.
- 4) M. Nagumo. Materials Science and Technology. 2004, Vol.20, pp.940-950.
- 5) K. Takai et al. Acta Materialia. 2008, Vol.56, pp.5158-5167.
- 6) T. Neeraj et al. Acta Materialia. 2012, Vol.60, pp.5160-5171.
- 7) N. Suzuki et al. Tetsu-to-Hagane. 1993, Vol.79, No.2, pp.227-232.
- 8) S. Yamasaki et al. Tetsu-to-Hagane. 1997, Vol.83, No.7, pp.454-459.
- 9) M. Kawamori et al. Corrosion Science. 2023, Vol.219, 111212.
- 10) M. Kawamori et al. ISIJ International. 2022, Vol.62, No.8, pp.1731-1740.
- 11) S. Takadate et al. Proceedings of the 70th Japan Conference on Materials and Environments. 2023-10-30/11-1. Japan Society of Corrosion Engineering. 2023, C-307.
- 12) J. Kinugasa et al. ISIJ International. 2016, Vol.56, No.3, pp.459-464.
- 13) T. Takimoto et al. Collected Abstracts of the 2023 Autumn Meeting of the Japan Inst. Metals and Materials. 2023-9-19/26. 2023, p.61.
- 14) T. Yasui et al. Materia Japan. 2024, Vol.63, No.1, pp.63-65.
- 15) M. Takeda et al. R&D Kobe Steel Engineering Reports. 2024, Vol.72, No.2, pp.33-37.
- 16) W. Urushihara et al. R&D Kobe Steel Engineering Reports. 2002, Vol.52, No.3, pp.57-61.
- 17) K. Hokazono et al. IOP Conference Series: Materials Science and Engineering. 2019, Vol.461, 012024.
- 18) K. Kagiya et al. CAMP-ISIJ. 2024, Vol.37, p.157.
- 19) J. Kinugasa et al. ISIJ International. 2021, Vol.61, No.4, pp.1071-1078.
- 20) J. Takahashi et al. Scripta Materialia. 2010, Vol.63, pp.261-264.
- 21) T. Pérez et al. Scripta Metallurgica. 1982, Vol.16, pp.161-164.
- 22) S. Evers et al. Science and Technology of Advanced Materials. 2013, Vol.14, 014201.
- 23) W. Krieger et al. Acta Materialia. 2018, Vol.144, pp.235-244.
- 24) M. Koyama et al. Scripta Materialia. 2017, Vol.129, pp.48-51.
- 25) J. Kinugasa et al. ISIJ International. 2021, Vol.61, No.4, pp.1091-1098.
- 26) M. Wang et al. Corrosion Science. 2007, Vol.49, pp.4081-4097.
- 27) A. Shibata et al. Acta Materialia. 2021, Vol.210, 116828.
- 28) M. Kawamori et al. ISIJ International. 2021, Vol.61, pp.1159-1169.